ChemElectroChem

Research Article
doi.org/10.1002/celc.202400354

Chemistry Europe
European Chemical Societies Publishing

www.chemelectrochem.org

Polyester-Polycarbonate Polymer Electrolytes Beyond $LiFePO_4$: Influence of Lithium Salt and Applied Potential Range

Isabell L Johansson,[a, b] Rassmus Andersson,[a] Johan Erkers,[a] Daniel Brandell,[a] and Jonas Mindemark*[a]

Rechargeable polymer-based solid-state batteries with metallic lithium anodes and $LiNi_xMn_yCo_{1-x-y}O_2$ (NMC)-based cathodes promise safer high-energy-density storage solutions than existing lithium-ion batteries, but have shown challenging to realize. The failure mechanisms that have been suggested for these battery cells have mostly been related to the use of a metallic lithium anode and formation of dendrites during cycling. Here, we approach the issue of using solid polymer electrolytes (SPEs) vs. NMC cathodes by employing a range of materials based on poly(ε-caprolactone-*co*-trimethylene carbonate) (PCL-PTMC) with different salts under various cycling conditions. It is seen that although the ionic conductivity of the electrolyte can be improved by exchanging the lithium salt, it does not immediately correlate to better cycling performance. However, increasing the temperature during battery cycling to improve the ion transport kinetics lowers the polarization of the battery cell and full capacity can be achieved at an upper voltage cut-off that is appropriate for the polymer electrolyte. For these electrolytes, the limit is demonstrated to be 4.4 V vs. Li^+/Li, and cycling with NMC-111 cathodes is thereby possible provided that the upper cut-off is limited to below this limit.

Introduction

Since their discovery in the mid-1970s,[1,2] solid polymer electrolytes have gone through much development. In the beginning of this research field, poly(ethylene oxide) (PEO), as well as poly(propylene oxide) (PPO), doped with different lithium, sodium and potassium salts, were investigated.[3] Due to several unfavorable properties of PPO, this polymeric material is now rarely employed, and PEO is dominating the field. However, the search for alternative host materials to PEO has continued, trying to overcome the numerous drawbacks of this material as a polymer electrolyte host, for example its high degree of crystallinity and low cationic transference number.[4]

Compared to liquid electrolytes, solid polymer electrolytes (SPEs) – which display advantages in terms of mechanical flexibility and safety – are still lacking in ionic conductivity. Since the main purpose of an electrolyte in a battery cell is to conduct ions back and forth between the electrodes during charge and discharge, this constitutes a major inadequacy which therefore limits the commercial development of polymer-based solid-state batteries. Aside from ionic conductivity, some additional deficiencies of polymer electrolytes commonly seen are: the cationic transference number, the electrochemical stability, the mechanical stability, and poor compatibility with high-voltage cathodes such as $LiNi_xMn_yCo_{1-x-y}O_2$ (NMC). Instead, the literature is dominated by cycling against $LiFePO_4$ cathodes.

One polymer host that could potentially serve as an alternative to PEO is poly(ε-caprolactone-*co*-trimethylene carbonate) (PCL-PTMC).[5] This polymer, which has been extensively explored in recent years, is a random copolymer composed of biocompatible monomers.[6] The synthesis of the polymer is generally performed through a simple ring-opening polymerization, and yields a high-molecular-weight, largely amorphous polymer. It is not only an excellent host to lithium ions but also sodium ions,[5,7] and shows comparatively high transference numbers and good battery cycling capabilities even at ambient temperature. It has, however, so far not shown the capability of long-term cycling against high-voltage cathodes such as NMC.

Considering the domination of PEO as an SPE host,[8] it is a common assumption that chemistries (salts, additives, polymer chain modifications, etc.) that are optimal or suitable for PEO, will also work for other polymer host materials. However, this has yet to be confirmed. One such example is the LiTFSI salt, first suggested for use with polymer electrolytes by Armand et al.,[9] and which has shown to form a strikingly good combination with PEO. The popularity of LiTFSI lies in its advantageous properties, especially over traditionally used salts

[a] I. L Johansson, R. Andersson, J. Erkers, D. Brandell, J. Mindemark
Department of Chemistry – Ångström Laboratory
Uppsala University
Box 538, SE-751 21 Uppsala, Sweden
E-mail: jonas.mindemark@kemi.uu.se

[b] I. L Johansson
Institute for Applied Materials – Energy Storage Systems (IAM-ESS)
Karlsruhe Institute of Technology (KIT)
Hermann-von-Helmholtz-Platz 1,
76344 Eggenstein-Leopoldshafen, Germany

Supporting information for this article is available on the WWW under https://doi.org/10.1002/celc.202400354

such as $LiPF_6$, e.g. lower toxicity, better thermal stability, and the large size of the anion causing the salt to dissociate more readily.[10] These properties should, in principle, also translate to other polymer hosts. At the same time, new and alternative lithium salts have been synthesized in recent years with both improved ionic conductivity and electrochemical stability.[11]

So far, the (electrochemical) compatibility between PCL-PTMC and other lithium salts than LiTFSI has not been studied, neither has a thorough evaluation of the cycling performance – its dependence on temperature and upper cut-off voltage – with NMC been performed. Exchanging the anion in the salt, or introducing alternative salts as additives, might allow a higher electrochemical stability in the electrolyte,[12–14] in addition to discovering new electrolyte compositions which have higher ionic conductivity and lower glass transition temperature. The exploration of different salts also renders a possibility to evaluate the obstacles for cycling NMC with PCL-PTMC, considering that TFSI degradation has been observed when cycling with NMC.[15] In principle, other salts can contribute with higher ionic conductivity, improved electrochemical stability or better film-forming abilities, and thereby rendering better cycling performance. Recently, the PCL-PTMC copolymer has also been used as a promising alternative to fluorinated binders in composite electrodes, further pointing at the versatility of this material as well as the importance of moving away from fluorinated compounds.[16] And although this polymer material shows high oxidative stability, further insight is needed on how to better cycle this material in high operating voltage cells.

In this work, we therefore study the behavior of a range of different salts (LiFSI, $LiBF_4$, $LiPF_6$, LiBOB, and LiDFOB) in PCL-PTMC, and report the electrochemical stability of these electrolytes using different electrochemical methods with varying cell set-ups. Furthermore, by changing the cycling conditions – such as cathode, temperature, and upper voltage cut-off – the relationship between the (kinetic) electrochemical stability and cycling performance is studied. In this context, the results of this study demonstrate that PCL-PTMC-based electrolytes, using both LiTFSI and LiBOB salts, are compatible with NMC cathodes with the right cycling conditions, and provides insight on appropriate measures to get SPEs to work successfully with high-voltage cathodes.

Results and Discussion

Just as there is a certain lack of diversity in polymer host materials used for SPEs, despite a recent upsurge in articles exploring alternative salts,[17–20] the lithium salt LiTFSI is still the most commonly used in polymer electrolytes. Similarly, only minor diversity can be found for salts used in liquid electrolytes, where – in contrast to SPEs – $LiPF_6$ dominates. $LiPF_6$ can be considered incompatible with solid polymer electrolytes because the salt decomposes readily at elevated temperatures, which are often required for polymer electrolytes to have sufficient ionic conductivity for battery cell cycling, and due to its sensitivity to water residues which are common after conventional casting techniques of especially polyethers.[21–23] In comparison, LiTFSI has a higher thermal stability, is less moisture sensitive, and decomposes into less toxic compounds.[24]

The main drawback with LiTFSI is that it cannot passivate aluminum, which is often used as current collector for the cathode (but seems to be less of a problem in solid-state cells). By comparison, the slightly smaller FSI anion has shown better abilities in this respect.[25,26] Some other potentially useful salts are the boron-containing $LiBF_4$, LiBOB and LiDFOB. Of these, $LiBF_4$ generally displays poor ionic conductivity and electrochemical stability and is therefore rarely used nowadays in any type of battery electrolyte.[27] Meanwhile, LiBOB is fluorine-free[28] and known for its film-forming ability at the electrode–electrolyte interface. The film-forming ability is also a property of the partially fluorinated LiDFOB, which can be considered as an intermediate of $LiBF_4$ and LiBOB. These salts, see Figure 1, have all been studied and used to some extent in several liquid electrolyte systems,[24,29,30] and also in multi-salt systems. However, equally comprehensive studies are not found for solid polymer electrolyte systems, which is also true for $LiPF_6$. While testing of these salts has been done for a few polymer host material systems,[31,32] they have yet to be introduced to the PCL-PTMC system.

When in contact with the $LiPF_6$ salt, the PCL-PTMC was found to have a noticeable change in color, from a light amber to an intense orange, both before and after solvent casting. Other than this, there were no major differences between the polymer electrolytes before, during, or after casting. However, this change that occurred with $LiPF_6$ in contact with PCL-PTMC is possibly reflected in the corresponding DSC thermogram,

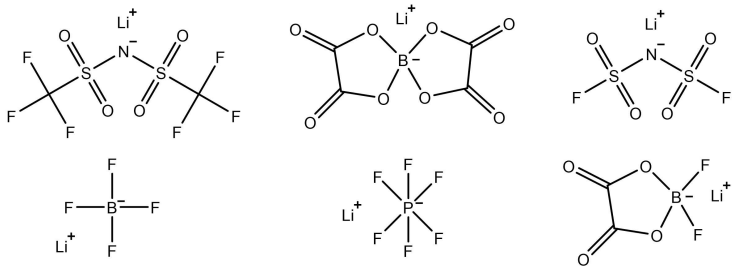

Figure 1. Molecular structures of the investigated lithium salts, from top left and onwards: lithium bis(trifluoromethanesulfonyl)imide (LiTFSI), lithium bis(oxalato)borate (LiBOB), lithium bis(fluorosulfonyl)imide (LiFSI), lithium tetrafluoroborate ($LiBF_4$), lithium hexafluorophosphate ($LiPF_6$), lithium difluoro(oxalato)borate (LiDFOB).

Figure 2a, where the $LiPF_6$-containing sample has a broader glass transition temperature compared to all other samples. The broadness of the glass transition could be affected by crystallinity or by the heat treatment of the sample during the DSC measurement. However, since all samples had the same heat treatment it is more likely that the widening of the T_g is due to partial PCL-PTMC degradation when in prolonged contact with the $LiPF_6$ salt, as $LiPF_6$ can spontaneously decompose to form highly reactive PF_5. Degradation of the polymer can change the dispersion of polymer chain lengths which in turn would affect the T_g.

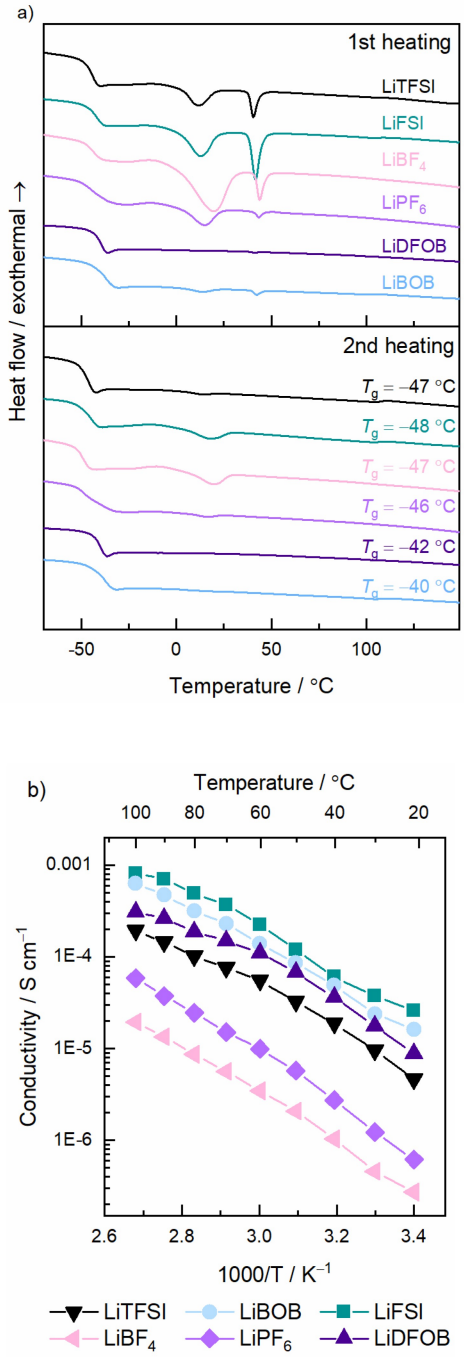

Figure 2. a) Heat flow of the differential scanning calorimetry measurements during the first heating scan and the second heating scan, with the T_g from the second heat scan. b) Arrhenius plot of the ionic conductivity of polymer electrolytes with different lithium salts; the lines are guides for the eye.

Generally, the PCL-PTMC host is fully amorphous when a reasonable amount of salt (≥28 wt% LiTFSI) has been added.[5] A slightly lower salt concentration is used in this work, and melting peaks can be seen for the electrolytes of LiTFSI and LiFSI during the first heating, but both are amorphous above room temperature and after any heat treatment, e.g. for EIS measurements. The DSC measurements showed that the electrolytes containing the borate salts, LiBOB and LiDFOB, are fully amorphous during the first and second heating scan, with no melting endotherm. For the electrolytes of $LiBF_4$ and $LiPF_6$, melting is seen in both the first and second heating scan. This could be due to the poor plasticizing ability of these salts in PCL-PTMC.

Despite that the glass transition temperature is an indication of the flexibility of the polymer chains, and that ionic conductivity is highly dependent on the chain flexibility, there is not always an absolute correlation between these properties. This is evident from the conductivity values for these electrolytes, shown in Figure 2b. Because the ratio of lithium ions to carbonyl oxygens in the PCL-PTMC host was kept constant for all salts – based on 20 wt% LiTFSI in PCL-PTMC and re-calculated for the other salts based on their molar mass – comparing the ionic conductivity for a fixed "molarity" (Li:C=O) of the polymer electrolytes is possible. However, it is not unlikely that the optimal ionic conductivity could be found at a different concentration of salt for all of these electrolytes. Interestingly, although LiTFSI is the most commonly used salt for solid polymer electrolytes, it does not have the highest ionic conductivity (at this concentration). The solid polymer electrolyte with LiFSI showed the highest ionic conductivity, followed by LiBOB, LiDFOB, and LiTFSI. The lowest ionic conductivity was found for the electrolytes of $LiBF_4$ and $LiPF_6$. The difference in ionic conductivity, especially between $LiBF_4$ and $LiPF_6$ and the other salts, could not be correlated either to their T_g or the coordination numbers obtained from vibrational spectroscopy analysis (see Figure S1).[33]

LiTFSI and LiFSI are structurally similar salts with good chemical stability and ability to dissolve in most polymer host materials; however, in the cyclic voltammetry measurements, see Figure 3, the SPEs featuring these two salts have the poorest performance in terms of electrochemical stability. The PCL-PTMC:LiFSI electrolyte is seemingly not stable in the potential range 3–5 V, as there is no potential span with zero current generation. Moreover, there are no signs of a stable plateau being reached between the first and second cycle, or for any of the five cycles (Figure S2), suggesting a lack of passivation for this electrolyte. While PCL-PTMC:LiTFSI also has a large current output, it is passivating by the second cycle. The $LiPF_6$ and LiBOB electrolytes, in turn, have the lowest amplitude in current generated throughout the cyclic voltammetry measurement, and PCL-PTMC:LiBOB appears to be the overall most stable. It is also important to note that the electrolyte based on $LiPF_6$ seems to be highly electrochemically reactive and generates current all through the potential scan 3–5 V vs. Li^+/Li, making it unsuitable for use under these conditions.

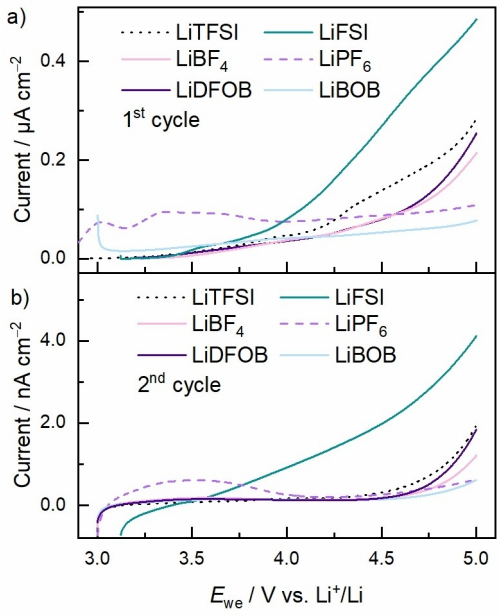

Figure 3. Anodic sweeps from the cyclic voltammetry measurements, showing the a) first and b) second sweep for each salt. The measurements were performed with a scan rate of 1 mV s^{-1}, at 60 °C.

However, as shown recently,[34–37] voltammetric measurements in conventional setups using inert electrodes do not necessarily reflect the electrochemical stability during galvanostatic cycling of a battery cell. Instead, it is recommended to shift the focus to the full electrochemical system of interest and analyze the behavior or the polymer electrolyte during actual galvanostatic cycling in a cell set-up that corresponds to a realistic situation. While this is generally more time-consuming than conventional voltammetric measurements, the acquired data is more relevant, and with careful design of the experiment, better knowledge can be obtained. Choices such as the cut-offs used, current density, and the cathode material will affect the response of the electrolyte.

Here, an initial evaluation of cycling performance with lithium iron phosphate (LFP) is done in order to give all the electrolytes a chance at showing their cyclability under gentle conditions that have previously yielded successful long-term battery cycling; see Figure S3. This is then followed by evaluating their performance in NMC-based cells, in which stable cycling is already known to be challenging to achieve. Cycling against LFP cathodes was done in the moderate voltage window of 2.8–3.8 V vs. Li$^+$/Li. The only experimental parameter which could be considered harsh is the high temperature of 60 °C; at this temperature the PCL-PTMC host is softened and malleable. The cycling performance with LFP is shown in Figure S3. Here, PCL-PTMC:LiTFSI showed the best performance, with a low polarization and high initial coulombic efficiency. The cell with PCL-PTMC:LiBOB electrolyte showed a similar cycling performance, albeit with a larger polarization. This high polarization does not correlate well with its comparatively high ionic conductivity, suggesting that the resistance in the battery cell rather stems from the formation of a resistive passivating film either on the metallic lithium or on the cathode, or both. The remaining electrolyte types displayed considerably worse battery performance. The cells with electrolytes containing LiFSI, $LiBF_4$ and LiDFOB had a low coulombic efficiency, a large polarization of ca. 0.2 V, and a specific capacity that is significantly below the theoretical capacity of LFP. The worst performance can be seen for cells containing electrolytes with $LiBF_4$ and $LiPF_6$; both of these showed large overpotentials and erratic cycling with soft short circuits, as seen by the brief drops in voltage, and voltage noise early on during the cycling. The poor electrochemical stability of PCL-PTMC:$LiPF_6$ shown in the LSV measurements (Figure 3) is thus reflected in poor cycling behavior in the LFP cells with this electrolyte. Borate salts are known for their film-forming abilities, and this is most likely the cause of the low initial coulombic efficiency and the high polarization during cycling, which is seen for both PCL-PTMC:LiBOB and PCL-PTMC:LiDFOB. Due to the slow kinetics of the film forming reactions, slow mass transport in polymer electrolytes, and retarded diffusion of anions to the reactive surface, these film-forming reactions might take several charge and discharge cycles to complete in SPE systems. This was seen for these two electrolytes during the LSV measurements – the other electrolytes displayed a noticeable reduction on current between the first and second cycle, but not the borate-containing counterparts which had a low current already during the first cycle. The problem seems less pronounced for PCL-PTMC:LiBOB, which has a fairly stable coulombic efficiency after ten cycles, while PCL-PTMC:LiDFOB showed a lot of voltage noise sporadically throughout the cycling.

An interesting occurrence for the cells containing PCL-PTMC:LiBOB and PCL-PTMC:LiDFOB is that they all displayed a drop in potential prior to the first charging step, see Figure S4, which coincides with the potential of LiBOB reduction.[38] This suggests that there were some spontaneous reactions occurring in these cells upon cell assembly, and most likely a highly resistive film is forming at the electrolyte-electrode interface on the side facing the lithium metal anode. Signs of the formation of this passivating film are also seen at the beginning of the first anodic sweep for PCL-PTMC:LiBOB, Figure 3a, where this electrolyte is drawing a current before any external potential is applied for the CV measurement. This drop in voltage was from the initial open circuit voltage of approximately 3 V vs. Li$^+$/Li, down to below 2 V vs. Li$^+$/Li.

Long-term cycling of polymer electrolytes containing LiTFSI with LFP electrodes has already been demonstrated for a lot of polymer host materials. One thing most solid polymer electrolytes have in common, though, is the difficulties when attempting to cycle against more high-voltage cathodes, such as NMC. The reason for this is not yet fully understood, with no consensus having been reached within the community, and is likely a tangled web of interconnecting factors. One hypothesis is that the mechanical stability of the polymer electrolytes is mostly at fault, implying that cycling can be performed as long as the polymer electrolyte is either cross-linked, thick enough, or if a spacer is incorporated into the cell to prevent flow of the electrolyte.[39–41] However, the electrochemical stability of the electrolyte is likely another important component. For example,

in a previous study focusing on improving the cycling of PCL-PTMC against NMC by zwitterionic additives,[42] it was found that the TFSI anion decomposed at the NMC cathode during galvanostatic cycling.

The cycling performance of the different electrolytes during galvanostatic cycling using an NMC-111 cathode, was evaluated with cut-off increase cell cycling (CICC) combined with intermittent current interruption (ICI). The ICI was combined with CICC in order to monitor the internal resistance during cycling to pinpoint changes in the electrolyte resistance to an increase in the upper cut-off. The CICC testing was performed to find the lowest upper cut-off that could be used to get a practically useful capacity out of the cells, and to find the highest upper cut-off that would not have a negative impact on the cycling performance due to degradation of the polymer electrolyte.[43,44]

For the NMC-111 electrode, the minimum requirement for the upper cut-off is 4.2 V vs. Li^+/Li in order to reach the redox reactions that are responsible for charge storage in this material. In Figure 4a, the cell with PCL-PTMC:LiTFSI is shown as an example of what the CICC measurement might look like, with an inset showing the cycling profile at some of the higher upper cut-offs. For this cell, there is a slow but steady increase of the polarization once the upper cut-off exceeds 4.2 V. Between the 56th and 66th cycle, there is only an increase of 0.2 V to the upper cut-off; however, the polarization increases by more than 1 V. This causes a reduction in the capacity as the upper cut-off is reached prematurely. By the 70th cycle, no capacity can be gained from the cell due to the high resistance.

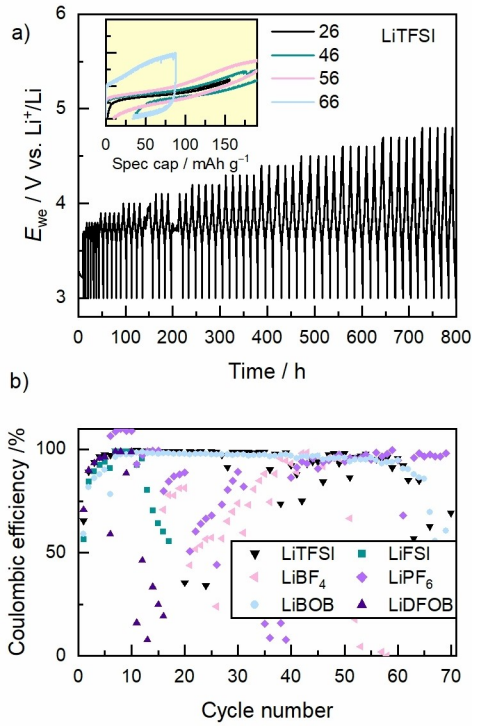

Figure 4. CICC measurements performed with the cell set-up Li^0|PCL-PTMC:salt|NMC111 and a current density of 5 μA cm^{-2}, at 60 °C. a) Full voltage profile featuring PCL-PTMC:LiTFSI during CICC, with an inset showing the cycling profiles of specific cycles. b) The coulombic efficiency of all investigated solid polymer electrolytes.

Other than the resistance, the coulombic efficiency (Figure 4b) is also used to determine the electrochemical stability of the cell during CICC measurements, where an unstable coulombic efficiency is an indication of detrimental side reactions. For PCL-PTMC:LiTFSI, unstable cycling can be seen from cycle 26 (4.2 V vs. Li^+/Li) and onwards.

If the resistance in the battery cell is only due to the bulk polymer electrolyte resistance, it can straight-forwardly be calculated from EIS measurements. However, all electrolytes had a higher resistance from ICI in the battery cell set-up than the bulk resistance which can be calculated based on the data from EIS; see Figure S5. This is due to reactions between the polymer electrolyte and the electrodes, which can lead to the formation of protective films forming on the interfaces or decomposition products with high resistance, or both. The differences between the expected resistance (bulk resistance only) and the actual resistance found in the cell using ICI, are especially large for PCL-PTMC:$LiBF_4$ and PCL-PTMC:$LiPF_6$, providing further confirmation that these electrolytes are unsuitable for cycling in this cell chemistry.

A fade in coulombic efficiency, increase in polarization and electrolyte resistance, is seen for both of the best-performing electrolytes (PCL-PTMC:LiTFSI and PCL-PTMC:LiBOB, Figure 4) around 4.4 V vs. Li^+/Li, suggesting that the inherent upper limit to the electrochemical stability of PCL-PTMC-based electrolytes under these conditions can be found at this voltage, and therefore that these electrolytes should be stable if the upper cut-off is kept below this value. This could explain why cycling with NMC is challenging for these electrolytes; the difficulty arises when the full capacity of the NMC-111 cannot be extracted at low upper cut-offs, forcing the use of a higher cut-off where the electrolyte itself is unstable. From the different galvanostatic measurement techniques and the CV measurements, it is clear that both PCL-PTMC:LiTFSI and PCL-PTMC:LiBOB are the most suitable to use in batteries. With some tuning, long-term cycling with NMC should likely be possible for these SPEs.

An important difference between liquid electrolytes and polymer electrolytes is that there are numerous academic studies and commercial products that have shown that it is possible to cycle liquid electrolytes with both LFP and NMC. Meanwhile, most published data on polymer electrolytes are limited to cycling with LFP. At the same time, a major difference between liquid electrolytes and polymer electrolytes is their ionic conductivity. Due to the faster ion transport in liquid systems compared to solid systems, the upper cut-off can be set to as low as 4.2 V vs. Li^+/Li when cycling NMC cells, with a maximum stability of 4.6 V vs. Li^+/Li of the NMC material itself.[45] It is probable that the issue in cycling solid state NMC cells is related to the lower ionic conductivity in the solid polymer electrolytes, but also the slower ion transport and high cut-offs that are used to compensate for high cell polarization.

With solid polymer electrolytes, increasing the operational temperature during battery cycling will increase the ionic conductivity of the electrolyte, reducing the polarization and the resistance of the cell. If the voltage cut-offs do not take this polarization into consideration, the cut-offs might be set too

low, resulting in a lower specific capacity being achieved as the cut-off is reached when the electrode is still at a low state-of-charge. To circumvent this, a higher upper cut-off voltage can be chosen, if the electrochemical stability of the electrolyte allows this.

Galvanostatic cycling with NMC was performed using PCL-PTMC:LiTFSI, PCL-PTMC:LiBOB, and PCL-PTMC:$LiPF_6$; both at 40 and 60 °C and for cut-off voltages of either 4.2 or 4.5 V vs. Li^+/Li. The $LiPF_6$-based SPE is interesting to evaluate because of its low ionic conductivity. As the results from CICC suggested, all cells show unstable cycling when the upper cut-off is set to 4.5 V vs. Li^+/Li regardless of the temperature, see Figure 5. On the other hand, the cycling is more stable with the lower cut-off of 4.2 V; see the coulombic efficiency of all cells in Figure S6. Moreover, 60 °C is required for both PCL-PTMC:LiTFSI and PCL-PTMC:LiBOB to reduce polarization enough to reach the redox plateau within the stability limit of the electrolyte, and to achieve a reasonable specific capacity. At this temperature, both cells have reduced polarization and increased specific capacity, suggesting that the limitation to cycling with NMC is primarily related to the ionic conductivity and faster ion transport at higher temperature. This is especially evident for PCL-PTMC:LiBOB, which has a higher resistance than PCL-PTMC:LiTFSI in the NMC cells, where the increase in temperature is accompanied by an increase in the specific capacity by over 100 mAh g^{-1} during the first cycle, as can be seen in the two lower rows in Figure 5. Although the LiBOB-based electrolyte has a higher ionic conductivity, according to EIS, in the cell set-up with NMC it consistently has a higher resistance than the cells with LiTFSI-based electrolyte. The high resistance in the cells with PCL-PTMC:LiBOB is likely due to the formation of a resistive passivating layer, and it is likely that LiBOB is more suitable as an electrolyte additive for its positive effect on the formation of passivation films in battery cells.

The appearance of the voltage noise during charging, most prominent in the PCL-PTMC:$LiPF_6$ cell at 60 °C and the PCL-PTMC:LiTFSI cell at 40 °C, both with an upper cut-off of 4.5 V could be attributed to either oxidative degradation of the cell components or to dendrites causing micro-shorts in the cells.[41] In these systems, the cause seems to be pointing toward issues with the electrochemical stability, since in both cases it is related to the higher upper cut-off that is used, as opposed to the temperature. As the PCL-PTMC becomes much softer at 60 °C compared to 40 °C, it should be more prone to dendrite penetration at the higher temperature.

Positive effects of using a combination of salts have already been shown for both liquid and polymer electrolytes.[46,47] Galvanostatic cycling of solid polymer electrolytes, using LiTFSI as the main conductive salt and LiBOB in additive amounts (r = 0.005 or 0.7 wt%), is shown in Figure 6. Here, the cell polar-

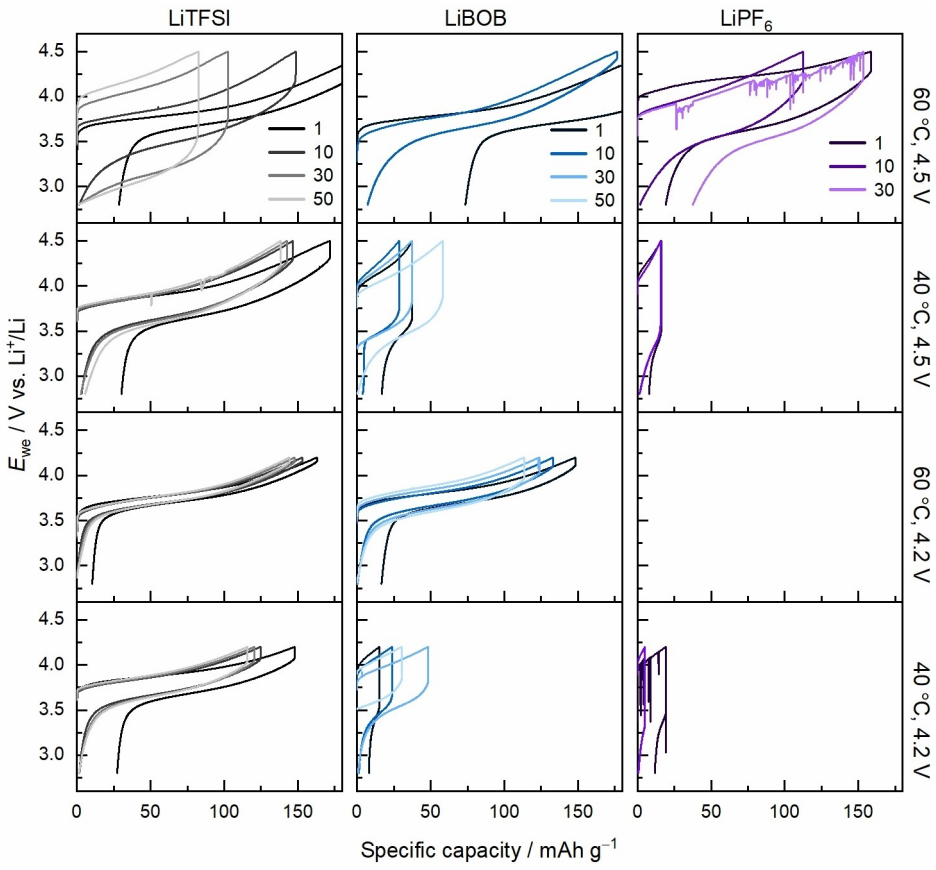

Figure 5. Galvanostatic cycling profiles of Li^0 | PCL-PTMC:salt | NMC-111, with a current density of 5 μA cm^{-2}. The cycling data is organized by operational temperature, either 60 °C or 40 °C, and by the upper cut-off, either 4.5 V or 4.2 V. The specific capacity for PCL-PTMC:$LiPF_6$ at 60 °C with the upper cut-off 4.2 V is close to zero.

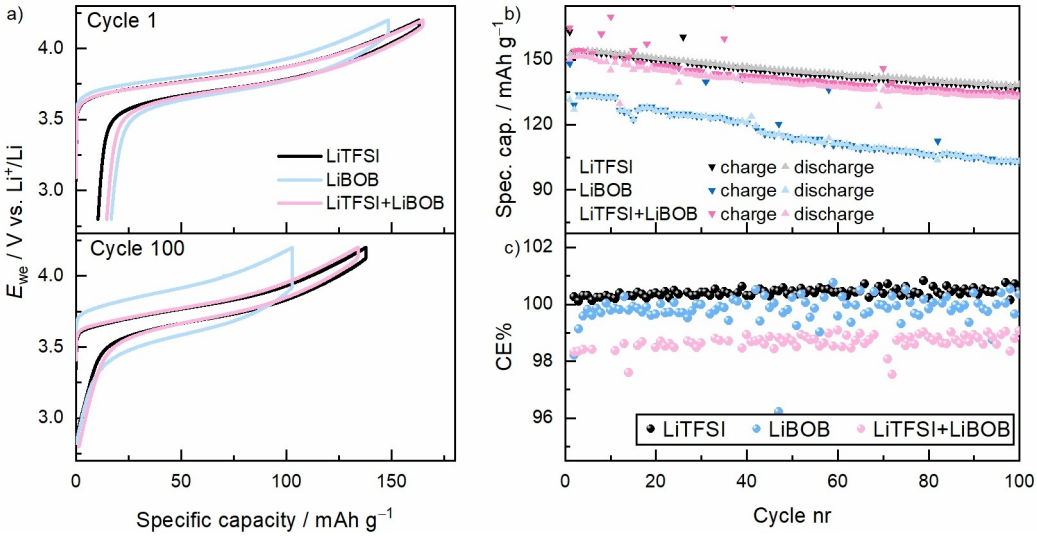

Figure 6. a) Galvanostatic cycling profile of the 1st and 100th cycle, b) the specific capacity during charging and discharging, and c) the coulombic efficiency. Galvanostatic cycling was performed on cells with Li^0|PCL-PTMC:salt|NMC, a current density of 5 μA cm^{-2} at 60 °C with an upper cut-off potential of 4.2 V vs. Li^+/Li. The electrolytes are PCL-PTMC:LiTFSI, PCL-PTMC:LiBOB, or PCL-PTMC:LiTFSI + LiBOB.

ization is lower when using the PCL-PTMC:LiTFSI + LiBOB electrolyte compared to the PCL-PTMC:LiBOB electrolyte. However, between the PCL-PTMC:LiTFSI and PCL-PTMC:LiTFSI + LiBOB there is less difference. Although a more prominent improvement can be seen in some studies when using LiBOB as an additive,[48–50] the addition here of LiBOB to the PCL-PTMC:LiTFSI electrolyte results primarily in a slight reduction and increase in spread of the coulombic efficiency (Figure 6c). While long-term cycling stability could possibly be provided by the inclusion of LiBOB additive, it is not apparent after only 100 cycles presented here. It is possible that even more effective additives are needed to properly passivate the electrodes, or optimized formation cycles, etc., but the issue appears to lie in the electrochemical stability of the material (PCL-PTMC:LiTFSI) itself. In Figure 5, it can also be seen that there is a large decrease in both the polarization and the charge capacity of the PCL-PTMC:LiBOB cell between the 1st and the 10th cycle. This could be an indication that a higher upper cut-off might be needed to properly oxidize the LiBOB in order to gain the benefits of its passivating layer. While the PCL-PTMC:LiBOB and PCL-PTMC:LiDFOB cells both show spontaneous reactions on the anode side, see Figure S4, it is the need for stability toward oxidation at the cathode side which limits the cycling with NMC electrodes.

Conclusions

This work has investigated several PCL-PTMC-based solid polymer electrolytes, in which the anion of the lithium salt has been varied (LiTFSI, LiFSI, $LiBF_4$, $LiPF_6$, LiBOB, and LiDFOB) in an attempt to evaluate how this affects the electrochemical stability, and what factors that control the galvanostatic cycling of these electrolytes in battery cells employing NMC-111 cathodes. The combined results from cyclic voltammetry and the different galvanostatic cycling methods in different cell set-ups show that the oxidative electrochemical stability of PCL-PTMC-based electrolytes is up to 4.4 V vs. Li^+/Li, which should render them compatible with NMC-type cathodes, provided that this potential is not exceeded. While both the LiFSI- and LiBOB-based electrolytes possessed a higher conductivity, PCL-PTMC:LiTFSI displayed the best cycling performance, showing that the bulk resistance of the electrolyte is not as important as the total resistance of the battery cell when the electrolyte is in contact with the electrodes. The performance of cells with PCL-PTMC-based electrolytes is dependent on a low cell resistance – which can be achieved at high temperature (≥ 60 °C) – and that the upper cut-off is kept below 4.4 V vs. Li^+/Li.

The inferior cycling performance in previous studies for these PCL-PTMC electrolytes with NMC could be correlated to both low ionic conductivity of the bulk electrolyte and high cell resistance due to either decomposition of the electrolyte or the formation of passivating films on the electrodes. While the film forming abilities of LiBOB and LiDFOB make them interesting for long-term cycling at demanding cycling conditions, the high resistances of the passivating films that they form make them unfit as the main conductive salt. Instead, it is suggested that LiBOB can be used as an additive for its film forming abilities. The formed film would then not be as thick due to the lower content of LiBOB, while it could still protect the surface from electrolyte decomposition. The use of additives in liquid electrolytes to prolong and improve cycling is a common practice, and should also be a viable option for SPEs.

Experimental

Polymer Electrolyte Preparation

Poly(ε-caprolactone-*co*-trimethylene carbonate) (average M_n = 200 000 g/mol) copolymer was synthesized according to the published procedure.[51,52] LiTFSI (BASF), LiBOB (ChemMetal), LiDFOB (Sigma-Aldrich), and $LiBF_4$ (Sigma-Aldrich, ≥98%) salts were dried at 120 °C under vacuum for 48 h, LiFSI (Solvionics, 99.9%) and $LiPF_6$ (Solvionics, 99.9%) were used as received. All handling, preparation, and cell assembly were done in an argon-filled glove box.

To facilitate comparison, the concentration of the salts as measured by the ratio of Li^+:C=O was kept constant at approximately $r = 0.05$, unless stated otherwise. This was based on the ratio of Li^+:C=O when using 20 wt% LiTFSI in PCL-PTMC, a composition which renders a reasonably high ionic conductivity.[5] Since the molar mass of the salts vary considerably, a strategy involving keeping the mass fraction of salt constant would have resulted in vastly different amounts of ions in relation to the coordinating carbonyl groups, with the risk of reaching the solubility limit for salts with low molar mass. The polymer and salt were homogeneously dissolved in acetonitrile (ACN; Sigma-Aldrich, 99.8%, anhydrous). The solvent was then removed in a vacuum oven at 30 °C for 20 h while vacuum was reduced from 200 mbar to 1 mbar, followed by 60 °C at 1 mbar for 40 h. The resulting polymer films were punched to a specific diameter and the thickness was measured.

Differential Scanning Calorimetry

A Mettler Toledo DSC 3+ system was used for differential scanning calorimetry (DSC) measurements in the temperature range from −80 to 150 °C with a cooling rate of 5 K min^{-1} and a heating rate of 10 K min^{-1}. The cooling and subsequent heating was performed twice for each sample in order to see the thermal properties of the polymer electrolytes before and after heat treatment.

Ionic Conductivity Measurements

Solid polymer electrolyte films with a diameter of 12 mm were sandwiched between two stainless steel blocking electrodes in CR2025 coin cells, using 50 μm PTFE films with an outer diameter of 19 mm and an inner diameter of 13 mm as a spacer inside the cell to evenly distribute the pressure on the electrolyte film. The cells were heated and annealed at 100 °C for 1 h the day before the measurements to improve the interfacial contact between the electrodes and the electrolyte. Electrochemical impedance spectroscopy (EIS) measurements were conducted on a Schlumberger SI 1260 Impedance/Gain-Phase Analyzer in a frequency range from 1 Hz to 10 MHz with an AC amplitude of 10 mV, in a temperature range of 30–100 °C with 10 °C steps, starting with a measurement at ambient temperature. The cells were kept at each test temperature for at least 30 min to reach thermal equilibrium. Fitting of the Nyquist plots was done in ZView to calculate the bulk ionic conductivity of the electrolyte.

Cell Assembly

For electrochemical characterization, pouch cells were assembled with Li-foil (China Energy Lithium co., 130 μm, 99.9%) with a 14 mm diameter, and solid polymer electrolyte, punched out to 16 mm diameter. All materials were used as-received and stored under inert conditions unless stated otherwise.

Cyclic Voltammetry

The electrochemical stability of the polymer electrolytes was studied by cyclic voltammetry on a Bio-Logic SP-240 potentiostat. The cells were assembled with a stainless steel foil (Sigma Aldrich, AISI 316 alloy, 25 μm thickness, 15 mm diameter, dried at 120 °C under vacuum for 12 h) as the working electrode, and scanned between 3.0 and 5.0 V vs. Li^+/Li at a scan rate of 1 mV s^{-1} at a temperature of 60 °C.

Galvanostatic Cycling and Cut-off Increase Cell Cycling (CICC)

The cathodes for galvanostatic cycling were composed of either LFP (TOB New Energy) or NMC–111 (Customcells) (75 wt%), conductive carbon black (C-NERGY™ Super C65, Imerys) (10 wt%) and the PCL-PTMC copolymer as binder (15 wt%). The electrodes were cut to a diameter of 12 mm and dried at 120 °C under vacuum for 12 h before use. The long-term cycling experiments on LFP were conducted with a current density of 5 μA cm^{-2} for both the lithiation and the delithiation. The voltage cut-offs were 3.8 and 2.8 V vs. Li^+/Li, at 60 °C. Cells with NMC cathodes were used for cut-off increase cell cycling (CICC) measurements[37] to study the electrochemical stability of the electrolytes in a cell set-up with a higher-voltage cathode. The cycling was conducted with a current density of 5 μA cm^{-2}, at 60 °C. The lower cut-off was 3.0 V, and the upper cut-off was increased with 0.1 V for every five cycles, from 3.7 to 5.0 V vs. Li^+/Li. The CICC measurements were supplemented with the intermittent current interruption (ICI) method,[53] with a 1 s current interrupting at 5 min intervals to monitor the resistance evolution during cycling.

Acknowledgements

This work has been financed through support from the ERC, grant no. 771777 FUN POLYSTORE, ECO^{2}LIB (European Union H2020 research and innovation programme under grant agreement no. 875514). We also acknowledge support from STandUP for Energy, and the Swedish Foundation for Strategic Research (project SOLID ALiBI, grant no. 139501338).

Conflict of Interests

The authors declare no conflict of interest.

Data Availability Statement

The data that support the findings of this study are available from the corresponding author upon reasonable request.

Keywords: all-solid-state batteries · electrolyte salts · polyester · polycarbonate · solid polymer electrolytes

[1] D. E. Fenton, J. M. Parker, P. V. Wright, *Polymer.* **1973**, *14*, 589. https://doi.org/10.1016/0032-3861(73)90146–8.
[2] A. Armand, M. Duclot, Composition composite de matériau d'électrode et d'un matériau élastomère à conduction ionique et électrode formée à partir de cette composition, Pat. 32976 No. 78, 1978.

[3] M. Armand, *Solid State Ionics.* **1983**, *9–10*, 745–754. https://doi.org/10.1016/0167-2738(83)90083–8.
[4] J. Mindemark, M. J. Lacey, T. Bowden, D. Brandell, *Prog. Polym. Sci.* **2018**, *81*, 114–143. https://doi.org/10.1016/j.progpolymsci.2017.12.004.
[5] J. Mindemark, B. Sun, E. Törmä, D. Brandell, *J. Power Sources* **2015**, *298*, 166–170. https://doi.org/10.1016/j.jpowsour.2015.08.035.
[6] E. Bat, B. H. M. Kothman, G. A. Higuera, C. A. van Blitterswijk, J. Feijen, D. W. Grijpma, *Biomaterials.* **2010**, *31*, 8696–8705. https://doi.org/10.1016/j.biomaterials.2010.07.102.
[7] C. Sångeland, R. Younesi, J. Mindemark, D. Brandell, *Energy Storage Mater.* **2019**, *19*, 31–38. https://doi.org/10.1016/j.ensm.2019.03.022.
[8] Z. Xue, D. He, X. Xie, *J. Mater. Chem. A* **2015**, *3*, 19218–19253. https://doi.org/10.1039/c5ta03471j.
[9] T. Yamamoto, M. Inami, T. Kanbara, *Chem. Mater.* **1994**, *6*, 44–50. https://doi.org/10.1021/cm00037a011.
[10] H. Zhang, M. Armand, *Isr. J. Chem.* **2021**, *61*, 94–100. https://doi.org/10.1002/ijch.202000066.
[11] L. Qiao, U. Oteo, M. Martinez-Ibañez, A. Santiago, R. Cid, E. Sanchez-Diez, E. Lobato, L. Meabe, M. Armand, H. Zhang, *Nat. Mater.* **2022**, *21*, 455–462. https://doi.org/10.1038/s41563-021-01190-1.
[12] K. Xu, *Chem. Rev.* **2014**, *114*, 11503–11618. https://doi.org/10.1021/cr500003w.
[13] C. F. N. N. Marchiori, R. P. Carvalho, M. Ebadi, D. Brandell, C. M. Araujo, *Chem. Mater.* **2020**, *32*, 7237–7246. https://doi.org/10.1021/acs.chemmater.0c01489.
[14] B. A. Fortuin, L. Meabe, S. R. Peña, Y. Zhang, L- Qiao, J. Etxabe, L. Garcia, H. Manzano, M. Armand, M. Martínez-Ibañez, J. Carrasco, *J. Phys. Chem. C* **2023**, https://doi.org/10.1021/acs.jpcc.2c07032.
[15] I. L. Johansson, C. Sångeland, T. Uemiya, F. Iwasaki, M. Yoshizawa-Fujita, D. Brandell, J. Mindemark, *ACS Appl. Energ. Mater.* **2022**, *5*, 10002–10012. https://doi.org/10.1021/acsaem.2c01641.
[16] H. Yeo, G. L. Gregory, H. Gao, K. Yiamsawat, G. J. Rees, T. McGuire, M. Pasta, P. G. Bruce, C. K. Williams, *Chem. Sci.* **2024**, *15*, 2371–2379. https://doi.org/10.1039/d3sc05105f.
[17] Z. Song, X. Wang, H. Wu, W. Feng, J. Nie, H. Yu, X. Huang, M. Armand, H. Zhang, Z. Zhou, *Journal of Power Sources Advances.* **2022**, *14*, 100088. https://doi.org/10.1016/j.powera.2022.100088.
[18] L. Qiao, U. Oteo, M. Martinez-Ibañez, A. Santiago, R. Cid, E. Sanchez-Diez, E. Lobato, L. Meabe, M. Armand, H. Zhang, *Nat. Mater.* **2022**, *21*, 455–462. https://doi.org/10.1038/s41563-021-01190-1.
[19] M. Martinez-Ibañez, E. Sanchez-Diez, U. Oteo, I. Gracia, I. Aldalur, H. B. Eitouni, M. Joost, M. Armand, H. Zhang, *Chem. Mater.* **2022**, *34*, 3451–3460. https://doi.org/10.1021/acs.chemmater.2c00285.
[20] B. A. Fortuin, L. Meabe, S. R. Peña, Y. Zhang, L. Qiao, J. Etxabe, L. Garcia, H. Manzano, M. Armand, M. Martínez-Ibañez, J. Carrasco, *J. Phys. Chem. C* **2023**, https://doi.org/10.1021/acs.jpcc.2c07032.
[21] H. Yang, G. V. Zhuang, P. N. Ross, *J. Power Sources* **2006**, *161*, 573–579. https://doi.org/10.1016/j.jpowsour.2006.03.058.
[22] C. Xu, B. Sun, D. Brandell, M. Hahlin, *J. Mater. Chem. A* **2014**, *2*, 7256–7264. https://doi.org/10.1039/c4ta00214h.
[23] D. Mankovsky, D. Lepage, M. Lachal, L. Caradant, D. Aymé-Perrot, M. Dollé, *Chem. Commun.* **2020**, *56*, 10167–10170. https://doi.org/10.1039/d0cc03556d.
[24] A. Mauger, C. M. Julien, A. Paolella, M. Armand, K. A. Zaghib, *Materials Science and Engineering R: Reports.* **2018**, *134*, 1–21. https://doi.org/10.1016/j.mser.2018.07.001.
[25] L. J. Krause, W. Lamanna, J. Summerfield, M. Engle, G. Korba, R. Loch, R. Atanasoski, *J. Power Sources* **1997**, *68*, 320–325. https://doi.org/10.1016/S0378-7753(97)02517–2.
[26] K. Matsumoto, K. Inoue, K. Nakahara, R. Yuge, T. Noguchi, K. Utsugi, *J. Power Sources* **2013**, *231*, 234–238. https://doi.org/10.1016/j.jpowsour.2012.12.028.
[27] R. Younesi, G. M. Veith, P. Johansson, K. Edström, T. Vegge, *Energy Environ. Sci.* **2015**, *8*, 1905–1922. https://doi.org/10.1039/c5ee01215e.
[28] G. Hernández, J. Mindemark, A. J. Naylor, Y. C. Chien, D. Brandell, K. Edstrom, *ACS Sustainable Chem. Eng.* **2020**, *8*, 10041–10052. https://doi.org/10.1021/acssuschemeng.0c01733.
[29] Q. Wang, L. Jiang, Y. Yu, J. Sun, *Nano Energy.* **2019**, *55*, 93–114. https://doi.org/10.1016/j.nanoen.2018.10.035.
[30] R. Weber, M. Genovese, A. J. Louli, S. Hames, C. Martin, I. G. Hill, J. R. Dahn, *Nat. Energy* **2019**, *4*, 683–689. https://doi.org/10.1038/s41560-019-0428-9.
[31] W. A. Henderson, *Macromolecules.* **2007**, *40*, 4963–4971. https://doi.org/10.1021/ma061866d.
[32] Q. Zhao, P. Chen, S. Li, X. Liu, L. A. Archer, *J. Mater. Chem. A* **2019**, *7*, 7823–7830. https://doi.org/10.1039/C8TA12008K.
[33] R. Andersson, G. Hernández, J. Mindemark, *Phys. Chem. Chem. Phys.* **2022**, *24*, 16343–16352. https://doi.org/10.1039/D2CP01904C.
[34] K. Xu, S. P. Ding, T. R. Jow, *J. Electrochem. Soc.* **1999**, *146*, 4172–4178. https://doi.org/10.1149/1.1392609.
[35] J. Kasnatscheew, B. Streipert, S. Röser, R. Wagner, I. Cekic Laskovic, M. Winter, *Phys. Chem. Chem. Phys.* **2017**, *19*, 16078–16086. https://doi.org/10.1039/C7CP03072J.
[36] A. Méry, S. Rousselot, D. Lepage, M. A. Dollé, *Materials.* **2021**, *14*, 3840. https://doi.org/10.3390/ma14143840.
[37] G. Hernández, I. L. Johansson, A. Mathew, C. Sångeland, D. Brandell, J. Mindemark, *J. Electrochem. Soc.* **2021**, *168*, 100523. https://doi.org/10.1149/1945-7111/ac2d8b.
[38] T. Melin, R. Lundström, E. J. Berg, *J. Phys. Chem. Lett.* **2024**, *15*, 2537–2541. https://doi.org/10.1021/acs.jpclett.4c00328.
[39] G. Homann, I. Stolz, K. Neuhaus, M. Winter, J. Kasnatscheew, *Adv. Funct. Mater.* **2020**, *30*, 1–8. https://doi.org/10.1002/adfm.202006289.
[40] L. Stolz, G. Homann, M. Winter, J. Kasnatscheew, *Materials Advances.* **2021**, *2*, 3251–3256. https://doi.org/10.1039/D1MA00009H.
[41] G. Homann, L. Stolz, J. Nair, I. C. Laskovic, M. Winter, J. Kasnatscheew, *Sci. Rep.* **2020**, *10*, 2–10. https://doi.org/10.1038/s41598-020-61373-9.
[42] I. L. Johansson, C. Sångeland, T. Uemiya, F. Iwasaki, M. Yoshizawa-Fujita, D. Brandell, J. Mindemark, *ACS Appl. Energ. Mater.* **2022**, *5*, 10002–10012. https://doi.org/10.1021/acsaem.2c01641.
[43] L. Seidl, R. Grissa, L. Zhang, S. Trabesinger, C. Battaglia, *Adv. Mater. Interfaces* 2100704 **2021**, 1–10. https://doi.org/10.1002/admi.202100704.
[44] L. Ma, M. Nie, J. Xia, J. R. Dahn, *J. Power Sources* **2016**, *327*, 145–150. https://doi.org/10.1016/j.jpowsour.2016.07.039.
[45] J. Kasnatscheew, M. Evertz, B. Streipert, R. Wagner, R. Klöpsch, B. Vortmann, H. Hahn, S. Nowak, M. Amereller, A. C. Gentschev, P. Lamp, M. Winter, *Phys. Chem. Chem. Phys.* **2016**, *18*, 3956–3965. https://doi.org/10.1039/c5cp07718d.
[46] J. Alvarado, M .A. Schroeder, T. P. Pollard, X. Wang, J. Z. Lee, M. Zhang, T. Wynn, M. Ding, O. Borodin, Y. S. Meng, K. Xu, *Energy Environ. Sci.* **2019**, *12*, 780–794. https://doi.org/10.1039/c8ee02601g.
[47] X. Lin, J. Yu, M. B. Effat, G. Zhou, M. J. Robson, S. C. T. Kwok, H. Li, S. Zhan, Y. Shang, F. Ciucci, *Adv. Funct. Mater.* 2010261 **2021**, 1–8. https://doi.org/10.1002/adfm.202010261.
[48] S. S. Zhang, *J. Power Sources* **2006**, *162*, 1379–1394. https://doi.org/10.1016/j.jpowsour.2006.07.074.
[49] A. M. Haregewoin, A. S. Wotango, B. J. Hwang, *Energy Environ. Sci.* **2016**, *9*, 1955–1988. https://doi.org/10.1039/c6ee00123h.
[50] Q. Zhao, P. Chen, S. Li, X. Liu, L. A. Archer, *J. Mater. Chem. A* **2019**, *7*, 7823–7830. https://doi.org/10.1039/C8TA12008K.
[51] A. P. Pêgo, A. A. Poot, D. W. Grijpma, J. Feijen, *J. Mater. Sci. Mater. Med.* **2003**, *14* 767–773. https://doi.org/10.1023/a:1025084304766.
[52] J. Mindemark, E. Törmä, B. Sun, D. Brandell, *Polymer.* **2015**, *63*, 91–98. https://doi.org/10.1016/j.polymer.2015.02.052.
[53] M. J. Lacey, K. Edström, D. Brandell, *Chem. Commun.* **2015**, *51*, 16502–16505. https://doi.org/10.1039/C5CC07167D.

Manuscript received: May 23, 2024
Version of record online: July 12, 2024